

Tunneling Evidence of Half-Metallic Ferromagnetism in $\text{La}_{0.7}\text{Ca}_{0.3}\text{MnO}_3$

J. Y. T. Wei,¹ N.-C. Yeh,¹ and R. P. Vasquez²

¹*Department of Physics, California Institute of Technology, Pasadena, California 91125*

²*Center for Space Microelectronics Technology, Jet Propulsion Laboratory, California Institute of Technology, Pasadena, California 91109*

(Received 19 May 1997)

Direct experimental evidence of half-metallic density of states (DOS) is observed by scanning tunneling spectroscopy on ferromagnetic $\text{La}_{0.7}\text{Ca}_{0.3}\text{MnO}_3$, which exhibits colossal magnetoresistance (CMR). Tunneling conductance data taken at 77 K, well below the Curie temperature $T_C \approx 260$ K, show close resemblance to the spin-split DOS spectrum calculated for the itinerant bands in the ferromagnetic state. The half-metallic spectral characteristics are absent in the paramagnetic state at room temperature, as well as in the undoped antiferromagnetic compound LaMnO_3 , which shows no CMR. These results directly implicate the half-metallic ferromagnetism in the phenomenon of CMR. [S0031-9007(97)04788-1]

PACS numbers: 75.50.Cc, 73.40.Gk, 75.10.Lp, 75.70.-i

The recent discovery of colossal magnetoresistance (CMR) in the perovskite manganites $\text{Ln}_{1-x}\text{A}_x\text{MnO}_{3-\delta}$ (Ln = trivalent rare earth ions, A = divalent alkaline earth ions) has rekindled interest in these compounds [1–6], with particular focus on the magnetic behavior of the conduction electrons. While the parent compound $\text{LnMnO}_{3-\delta}$ is known to be an antiferromagnetic (AFM) insulator with Néel temperature $T_N \sim 150$ K, the doped compounds in the nominal regime $0.2 < x < 0.5$ behave as paramagnetic (PM) insulators at high temperatures and ferromagnetic (FM) metals below the Curie temperature T_C , near which the magnetoresistance peaks. The FM ordering has been attributed to the double-exchange interaction between the valence electronic states of $\text{Mn}^{3+}\text{-O}^{2-}\text{-Mn}^{4+}$ [7–10]. The double-exchange mechanism is also believed to be responsible for the occurrence of CMR [3,11,12], in conjunction with the effects of lattice distortion in the manganites [13]. A direct consequence of the double-exchange and the lattice distortion is a large spin splitting of the conduction band into majority and minority subbands in the FM state [14]. These subbands are separated by the on-site Hund's rule energy, which is about several eV's, depending on the A-site doping. The large spin splitting renders the conduction band half-metallic, i.e., with the ground-state electrons nearly perfectly spin polarized [15].

Theoretically, half-metallic FM in the CMR manganites has been justified by *ab initio* band structure calculations. Hamada, Sawada, and Terakura used linear augmented plane wave methods to study LaMnO_3 and $\text{La}_{0.5}\text{Ba}_{0.5}\text{MnO}_3$, showing their respective ground states to be AFM insulating and FM half-metallic [16]. Satpathy, Popovic, and Vukajlovic reached similar conclusions about the $\text{La}_{1-x}\text{Ca}_x\text{MnO}_3$ system using density-functional techniques [17]. Pickett and Singh also performed calculations of the $\text{La}_{1-x}\text{Ca}_x\text{MnO}_3$ system, using the local spin-density approximation [14]. This latter work demonstrated the im-

portance of lattice distortion induced by both cation size-mismatch and the Jahn-Teller effect, in enhancing the FM exchange splitting of the itinerant bands.

Experimentally, both optical and transport studies have provided evidence in support of half-metallic FM in the CMR manganites. Okimoto *et al.* reported temperature dependent optical conductivity spectra on $\text{La}_{1-x}\text{Sr}_x\text{MnO}_3$ ($x = 0.175$) single crystals, consistent with a fully spin-polarized conduction band associated with exchange splitting [18]. Hwang *et al.* reported temperature dependent magnetoresistance in polycrystalline $\text{La}_{1-x}\text{Sr}_x\text{MnO}_3$ ($x = \frac{1}{3}$), attributable to spin-polarized tunneling between field-aligned half-metallic grains [19]. Sun *et al.* demonstrated large field-induced resistance modulation in trilayer devices based on $\text{La}_{1-x}\text{Sr}_x\text{MnO}_3$ and $\text{La}_{1-x}\text{Ca}_x\text{MnO}_3$ ($x = \frac{1}{3}$), in accordance with the model of spin-polarized tunneling through a half-metal/insulator/half-metal junction [20].

Despite the evidence supporting half-metallic FM in the CMR manganites, detailed understanding of the electronic structure involved requires direct measurement of the electronic density of states (DOS). Tunneling spectroscopy has been known to provide a sensitive probe of the DOS [21], particularly if the tunneling is into a many-body system characterized by a renormalized quasiparticle dispersion [22,23]. This Letter reports direct evidence of half-metallic DOS by scanning tunneling spectroscopy on an epitaxial film sample of FM $\text{La}_{0.7}\text{Ca}_{0.3}\text{MnO}_3$ (LCMO). At 77 K, well below T_C , the tunneling conductance data exhibit pronounced peak structures, bearing close resemblance to the half-metallic DOS spectrum calculated for the itinerant bands in FM $\text{La}_{1-x}\text{Ca}_x\text{MnO}_3$. The half-metallic spectral characteristics are absent at room temperature in the PM state, as well as in the undoped compound LaMnO_3 (LMO) which shows no CMR. These observations directly implicate the half-metallic FM, as a combined effect of double-exchange and lattice distortion, in the phenomenon of CMR.

Epitaxial film samples of LCMO and LMO were grown by pulsed laser deposition on (100) LaAlO₃ (LAO) substrates using stoichiometric targets. The films were 100 nm thick and grown at 700 °C in 100 mTorr of oxygen, and subsequently annealed at 900 °C in 1 atm oxygen for several hours. X-ray diffraction and photoelectron spectroscopy confirmed the samples to be stoichiometric, single phase, and epitaxial [24]. Optical measurements on the LCMO film indicated phonon modes consistent with those obtained on bulk LCMO of the same chemical composition [25]. The Curie temperature for the LCMO film was determined to be $T_C \approx 260$ K by measuring the spontaneous magnetization versus temperature with a SQUID magnetometer. Details of the sample synthesis and characterization are given in Refs. [26–28].

The surface quality of our films was inferred from the spectroscopic measurements by x-ray photoelectron spectroscopy (XPS) and the topographic images by scanning tunneling microscopy (STM). The XPS measurements were made at room temperature under ultrahigh vacuum for photoemission normal to the film surface [24]. Spectra taken on both as-grown and Br-etched samples show the core level binding energy peaks expected for each compound with very low contaminant signals, demonstrating the surface cleanliness of our films. The STM surface topographs were made in constant-current mode at ~ 1 nA with a Pt-tip biased at ~ -2 V [26]. An example of the STM image (150×150 nm², 5 nm grey scale) for the LCMO film is given in Fig. 1, showing atomically smooth “rice-paddy” terraces with unit-cell step heights. Such images were obtainable at both room temperature and 77 K, in either high vacuum or ultrapure helium gas, attesting to the high surface quality of our films.

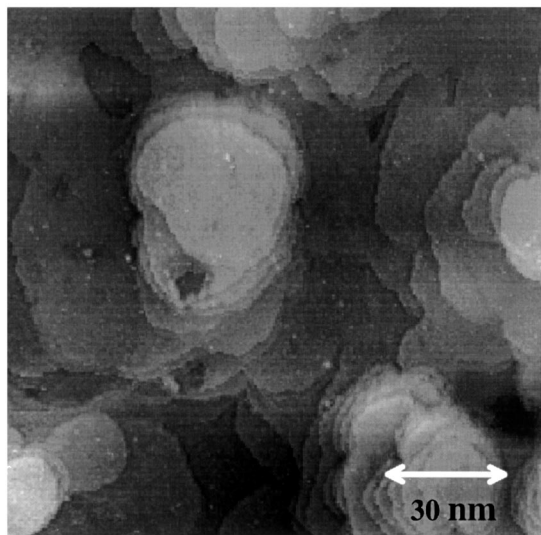


FIG. 1. STM topography of the LCMO epitaxial film grown on LAO substrate. The image is 150×150 nm² in size and 5 nm in grey scale, showing atomically smooth rice-paddy terraces with unit-cell step heights.

Scanning tunneling spectroscopy was performed on the same LCMO and LMO films which had been fully characterized with the measurements described above. The tunneling spectra were taken by momentarily interrupting the STM feedback during a scan and measuring the tunneling current as a function of the sample bias voltage. Typical junction impedance was ~ 1 G Ω . The measured spectra were highly reproducible, showing little variation with junction impedance (see below) and position on the sample, in either high-vacuum or ultrapure helium gas. The current versus voltage I - V data were converted numerically into the normalized tunneling conductance $(dI/dV)/(I/V)$, which gives a measure of the density of states [21]. Here, the normalization is necessary to divide out the voltage dependence inherent in the STM transmission probability, which can be estimated by $I/V \equiv \int_{-\infty}^{\infty} [I/V'] \exp\{-\frac{|V'-V|}{\Delta V}\} dV'$ using the weighting function $\exp\{-\frac{|V'-V|}{\Delta V}\}$ with an adjustable spectral width ΔV [29]. In the presence of an energy gap, where both I and dI/dV are zero, a finite ΔV of typically the gap size is needed to smooth out numerical divergences in the $(dI/dV)/(I/V)$ spectrum [29,30].

Figure 2(a) shows the $(dI/dV)/(I/V)$ data plotted versus V for LCMO in the FM state at 77 K. Pronounced peaks are present at $\sim \pm 1.75$ V, with half-height widths of ~ 1 V. These peaks can be compared with the exchange-split, spin-polarized peaks in the DOS spectrum calculated by Pickett and Singh for the itinerant Mn $3d$ and O $2p$ bands in FM La_{1-x}Ca_xMnO₃ ($x = 0.25$) [14]. These half-metallic peaks are clearly absent at room temperature for LCMO in the PM state [Fig. 3(a)], where there is no exchange interaction among the conduction electrons. The peaks also do not appear in the undoped LMO [Figs. 2(b) and 3(b)], which is an AFM insulator with $T_N \approx 150$ K and shows no CMR. These observations directly correlate the half-metallic FM with the occurrence of CMR in the doped manganites. The energy separation between the half-metallic peaks provides a measurement of the intra-atomic Mn d -electron exchange splitting ΔE , which is simply related to the on-site Hund's rule energy in the double-exchange model [7–11]. Our data indicate $\Delta E \approx 3.5$ eV, in close agreement with the value calculated for FM La_{1-x}Ca_xMnO₃ ($x = 0.25$) [14].

Also noticeable in the tunneling data for LCMO at 77 K [Fig. 2(a)] is a gap structure with sharp edges at $\sim \pm 0.5$ V. Such a gap is present as well in the data for LMO at 77 K [Fig. 2(b)], although slightly smaller at $\sim \pm 0.35$ V. For LMO, this could be evidence for an insulator gap resulting from structural distortion induced by both the cation size-mismatch and the Jahn-Teller effect [14]. For LCMO, such evidence would be consistent with models for CMR involving polaron conduction [13]. Band structure calculations for LMO indicate a direct gap of ~ 0.7 eV [14], which is close to the optical gap of ~ 1 eV measured by Arima *et al.*

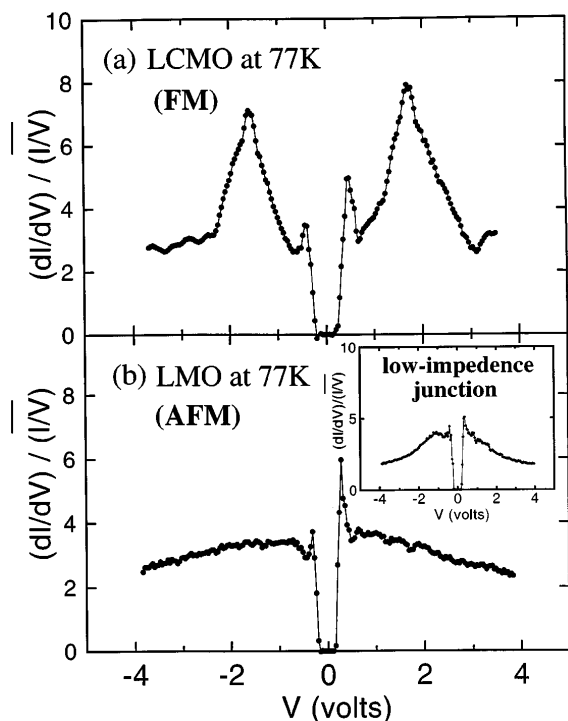


FIG. 2. STM spectroscopy data taken at 77 K, well below the Curie temperature, plotted as the normalized conductance $(dI/dV)/(I/V)$ versus the sample bias voltage V . (a) The LCMO film in the FM state, showing pronounced peaks at $\sim\pm 1.75$ V and a gap structure with edges at $\sim\pm 0.5$ V. (b) The LMO film in the AFM state, showing no peaks but similar gap features at $\sim\pm 0.35$ V. Data for a low-impedance (~ 1 M Ω) junction is included as an inset in (b), showing the same gap features and a slight hump at ~ -1 V but also no pronounced peak structures relative to the spectral background.

[31]. Our own transport measurements on the LCMO sample used in this experiment suggest a polaron binding energy (relative to the Fermi level) of ~ 0.35 eV [27], which compares well with the calculated Jahn-Teller coupling energy [13]. These theoretical and experimental results are in general agreement with the energy gaps we observed by tunneling: ~ 0.7 eV in AFM LMO and ~ 1 eV in FM LCMO.

It is important to note that the basic spectral behaviors we observed are insensitive to the junction impedance. This is demonstrated by the low-impedance (~ 1 M Ω) tunneling data for AFM LMO [inset in Fig. 2(b)], showing the same gap but clearly no peak structures as in the high-impedance (~ 1 G Ω) data plotted in the main figure. The slight hump at ~ -1 V in the low-impedance data may reflect additional spectral features due to AFM exchange splitting of the DOS [14], but nowhere as pronounced, relative to the spectral background, as the half-metallic exchange-split peaks in the case of FM LCMO [Fig. 2(a)]. This basic spectral insensitivity to junction impedance indicates reasonable material homogeneity between the surface and the bulk of our films, at least in the

vacuum-gap scenario, since the tunneling depth is sensitive to the gap thickness.

It is also interesting to note that the room temperature tunneling spectra for LCMO and LMO [Figs. 3(a) and 3(b)] show only a weak gaplike behavior, with $(dI/dV)/(I/V)$ dipping to its minimum value of unity near zero bias [30]. This behavior could be interpreted in terms of the band-structure cancellation effect first described by Harrison [32]. In the PM state, the electronic dispersion $\xi_{\mathbf{k}}$ (ξ is the energy and \mathbf{k} is the wave vector) is not renormalized by any many-body correlations, thus making the DOS ($\sim \partial k / \partial \xi$ in one dimension) prone to cancellation by the group velocity ($\sim \partial \xi / \partial k$) inherent in the tunneling matrix element [23]. In contrast, the DOS in a magnetically ordered state is renormalized by the exchange interaction, thus circumventing the group-velocity cancellation which would prevent any gap structures in the DOS from clearly showing up in the tunneling spectra. Therefore, the dip features present in our room temperature data are not inconsistent with the existence of an energy gap seen in both LCMO and LMO at 77 K. On the other hand, the spin-split peak structure seen in LCMO at 77 K is clearly absent in the room temperature spectra, consistent with it being unique to the FM state of LCMO and a distinct signature of half-metallic FM.

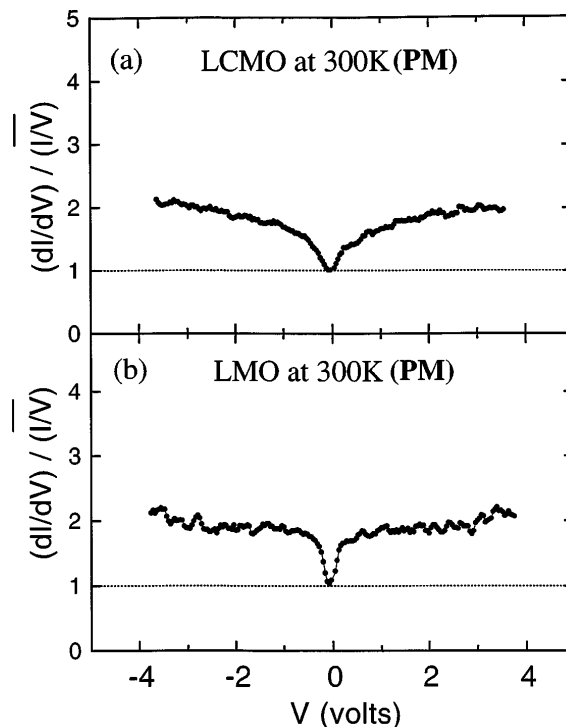


FIG. 3. STM spectroscopy data taken at 300 K, well above the Curie temperature, plotted as the normalized conductance $(dI/dV)/(I/V)$ versus the sample bias voltage V . (a) The LCMO film in the PM state, and (b) is the LMO film in the PM state. Both spectra show a weak gaplike behavior, dipping to its minimum value of unity (indicated by the dotted baseline) near zero bias (see Ref. [30]).

In summary, we have observed direct evidence, for the first time, of half-metallic density of states in ferromagnetic $\text{La}_{0.7}\text{Ca}_{0.3}\text{MnO}_3$ by scanning tunneling spectroscopy. The normalized tunneling conductance data show pronounced spectral peaks which can be identified as the exchange-split spin-polarized density-of-states peaks for the itinerant band electrons. These half-metallic spectral characteristics are absent at room temperature in the paramagnetic state, as well as in the undoped antiferromagnetic compound LaMnO_3 . Our results directly implicate the half-metallic ferromagnetism, as a combined effect of double-exchange and lattice distortion in the doped manganites, in the phenomenon of colossal magnetoresistance.

The research at Caltech is supported by the Packard Foundation and the National Aeronautics and Space Administration, Office of Space Science (NASA/OSS), and the Caltech President's Fund. Part of the research was performed by the Center for Space Microelectronics Technology, Jet Propulsion Laboratory, Caltech, and was sponsored by NASA/OSS.

-
- [1] G.H. Jonker and J.H. van Santen, *Physica (Utrecht)* **16**, 337 (1950).
- [2] E.O. Wollan and W.C. Koehler, *Phys. Rev.* **100**, 545 (1955).
- [3] C.W. Searle and S.T. Wang, *Can. J. Phys.* **47**, 2703 (1969).
- [4] R. von Helmolt *et al.*, *Phys. Rev. Lett.* **71**, 2331 (1993).
- [5] S. Jin *et al.*, *Science* **264**, 413 (1994).
- [6] P.E. Schiffer *et al.*, *Phys. Rev. Lett.* **75**, 3336 (1995).
- [7] C. Zener, *Phys. Rev.* **82**, 403 (1951).
- [8] P.W. Anderson and H. Hasegawa, *Phys. Rev.* **100**, 675 (1955).
- [9] J. Goodenough, *Phys. Rev.* **100**, 564 (1955).
- [10] P.-G. de Gennes, *Phys. Rev.* **118**, 141 (1960).
- [11] K. Kubo and N. Ohata, *J. Phys. Soc. Jpn.* **33**, 21 (1972).
- [12] N. Furukawa, *J. Phys. Soc. Jpn.* **63**, 3214 (1994).
- [13] A.J. Millis, P.B. Littlewood, and B.I. Shraiman, *Phys. Rev. Lett.* **74**, 5144 (1995); A.J. Millis, B.I. Shraiman, and R. Mueller, *Phys. Rev. Lett.* **77**, 175 (1996).
- [14] W.E. Pickett and D.J. Singh, *Phys. Rev. B* **53**, 1146 (1996).
- [15] V. Yu. Irkhin and M.I. Katsnel'son, *Sov. Phys. Usp.* **37**, 659 (1994).
- [16] N. Hamada, H. Sawada, and K. Terakura, in *Spectroscopy of Mott Insulators and Correlated Metal*, edited by A. Fujimori and Y. Tokura (Springer-Verlag, Berlin, 1995), pp. 95–105.
- [17] S. Satpathy, Z.S. Popovic, and F.R. Vukajlovic, *Phys. Rev. Lett.* **76**, 960 (1996).
- [18] Y. Okimoto *et al.*, *Phys. Rev. Lett.* **75**, 109 (1995).
- [19] H.Y. Hwang *et al.*, *Phys. Rev. Lett.* **77**, 2041 (1996).
- [20] J.Z. Sun *et al.*, *Appl. Phys. Lett.* **69**, 3266 (1996).
- [21] For reviews, see R.M. Feenstra, *Surf. Sci.* **299/300**, 965 (1994); R.J. Hamers, *Annu. Rev. Phys. Chem.* **40**, 531 (1989); V.A. Ukraintsev, *Phys. Rev. B* **53**, 11176 (1996).
- [22] G.D. Mahan, *Many Particle Physics* (Plenum, New York, 1990).
- [23] E.L. Wolf, *Principles of Electron Tunneling Spectroscopy* (Oxford University Press, New York, 1985); C.B. Duke, *Tunneling in Solids* (Academic Press, New York, 1969).
- [24] R.P. Vasquez, *Phys. Rev. B* **54**, 14938 (1996).
- [25] A.V. Boris *et al.*, *J. Appl. Phys.* **81**, 5756 (1997).
- [26] N.-C. Yeh *et al.*, *J. Appl. Phys.* **81**, 5499 (1997).
- [27] N.-C. Yeh *et al.*, *J. Phys. Condens. Matter* **9**, 3713 (1997).
- [28] N.-C. Yeh *et al.*, *Epitaxial Oxide Thin Films III* (Materials Research Society, Pittsburgh, PA, 1997).
- [29] R.M. Feenstra, *Phys. Rev. B* **50**, 4561 (1994); J.A. Stroscio, R.M. Feenstra, and A.P. Fein, *Phys. Rev. Lett.* **57**, 2579 (1986); P. Martensson, and R.M. Feenstra, *Phys. Rev. B* **39**, 7744 (1989).
- [30] Note that, as a result of the numerical smoothing in I/V , the normalized conductance $(dI/dV)/(\overline{I/V})$ is not required to approach unity at zero bias, as one might expect from L'Hôpital's rule. The spectral broadening renders $\overline{I/V}$ finite even near zero bias, thus allowing $(dI/dV)/(\overline{I/V})$ to be zero wherever dI/dV is zero, especially near the gap edges where I/V tends to approach zero faster than dI/dV . This is clearly the case in the low-temperature data (Fig. 2), where a vanishing zero bias $(dI/dV)/(\overline{I/V})$ is physically consistent with the absence of states inside the energy gap. Only in the limit of zero gap size, as the ΔV needed for smoothing shrinks to zero, the spectral weighting $\exp\{-\frac{|V'-V|}{\Delta V}\}$ becomes a delta function, and $\overline{I/V}$ reduces to I/V , does the normalized conductance $(dI/dV)/(\overline{I/V}) \rightarrow 1$ for $V \rightarrow 0$, as is evident in the high-temperature data (Fig. 3).
- [31] T. Arima *et al.*, *Phys. Rev. B* **48**, 17006 (1993).
- [32] W. A. Harrison, *Phys. Rev.* **123**, 85 (1961).